Reviewer # 1

Summary:

Radar forward operators transform the model's prognostic variables to the observed radar variables and are crucial tools in a number of applications including model evaluation, retrieval development, and data assimilation. The manuscript presents a newly developed radar forward operator based on the T-matrix method for calculating scattering amplitudes. The radar forward operator uses a non-spheroid hydrometeor model, namely the Chebyshev-shaped model to characterize the raindrops. The difference between the Chebyshev-shaped model and the spheroid model for calculating raindrop radar variables was compared in different single-moment (SM) schemes. However, the effect of the Chebyshev-shaped model on radar variables may only be notable in the presence of extremely large raindrops.

Overall, the topic of the manuscript is scientifically interesting and relevant. The presentation of the paper is reasonably good. The writing quality is fine and clear. I do have several comments below which I think translate into a recommendation for major revisions. I do not think there is anything fundamentally wrong with the manuscript, but considerable clarification on some points is needed as well as an expansion of the case results on polarimetric radar variables.

Response: We appreciate the reviewer's positive feedback and constructive comments on improving the manuscript.

We have implemented six typical single-moment (SM) drop size distribution (DSD) models into the radar operator and found that the Chebyshev raindrop model shows noticeable differences of bulk scattering properties (compared to the spheroid model) for electromagnetic waves of millimeter-wavelength at zenith and nadir observation geometries. This difference is more prominent for continental DSD models (e.g., Wang2016) with larger drops. The reflectivity contrast between zenith and nadir viewing angles can be as high as 4-5 dB, as illustrated in Figure 1. Such a difference is non-existent for spheroid raindrops with reflectance symmetry. Given the lower uncertainties in simulating reflectivity of liquid phase compared to solid and melting phases, such a difference deserves attention in specific applications such as comparing data from ground-based and spaceborne radar observations.

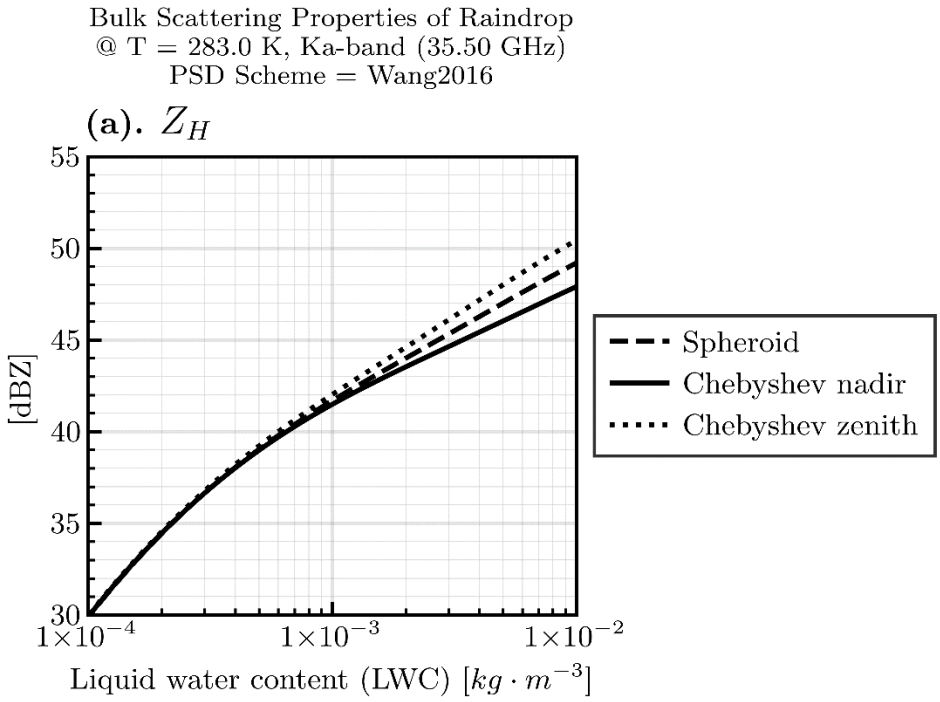

Figure 1: The BSP of raindrop for Wang2016 PSD scheme temperature=283K, elevation=1 deg., and Ka-band (35. 5GHz) for spheroid and Chebyshev shape raindrop at nadir (elevation=-90 deg.) at zenith (elevation=90 deg.)

Actually, this study not only presents an alternative raindrop particle model in the forward radar operator, but also demonstrates the capability for ZJU-AERO to handle particle models with unprecedented complexities.

Additionally, due to the current length of this manuscript, we have included a simulation case of ground-based polarimetric radar variables in the user manual of the software (released with the software package) rather than adding it to the research paper. This simulation case effectively showcases that our forward radar operator works properly in simulating polarimetric ground-based radar variables.

For further details, please refer to the specific responses provided below.

Major comments:

1. In the ABSTRACT and INTRODUCTION, the authors claimed the main purpose of developing this radar forward operator is to assimilate the polarimetric radar variables. However, it is not clarified in what follows that the operator has the potential to be able to be used for assimilating polarimetric radar. For the data assimilation purpose, the simplicity and efficiency of the radar forward operator are necessary. How computationally efficient is this radar forward operator? The variational method requires the tangent linear (TL) and adjoint (AD) operators, so whether this complex forward operator can be easily linearized. If the goal is to use it for data assimilation, then the manuscript needs to include sufficient discussion about the relevant

aspects (advantages, limitations, and alternatives) of the radar forward operator.

Response:

Thanks for the suggestions.

(1) We have added specifications on the techniques used to accelerate the forward simulations in section 2:

"The above procedures of steps 1-5 (excluding the first step transferring the model state data from model grid to regular grid) are independent for each single beam, which guarantees the top-level scalability of the forward operator. Therefore, we are using the shared-memory python parallel library (multiprocessing) to speed up the simulation.
In addition, for those computationally intensive tasks (such as the trilinear interpolation in step 3), we are employing the technique of mixed programming (building C/Fortran-extensions that interface with python scripts) to further accelerate the computation.
The performance of the forward operator is generally satisfactory: ZJU-AERO can complete a ground-base station volume scan with 9 Plan Position Indicator (PPI) sweeps in 2 minutes on a modern laptop with a 6-core CPU (i7-10750H) if online size distribution integration is performed and the operator takes Level-B single scattering property database as input. If Level-C bulk scattering property database is used, such a volume PPI scan can be completed even faster (in 30s). Such efficiency can support data assimilation purposes, while also preserving flexibility for research purposes."

(2). The first application of ZJU-AERO in CMA-GFS / MESO is planned to be used with the Bayesian approach. The data assimilation framework of the Bayesian method involves clustering the characteristics of atmosphere profiles using a statistic method. It only requires forward relationships that maps model states to the observational space, thus not needing tangent-linear (TL) or adjoint (AD) operators.

The development of future hydrometeor control variables in CMA-GFS/MESO by the variational method also shows promise. However, this approach requires more work in linearizing ZJU-AERO.

The direct linearization of this forward operator could be complex. One approach to circumvent the difficult could be to first find polynomial fits to the level-C bulk scattering database, and then compute the derivatives of those fits with respect to the input parameters (e.g., temperatures, mass concentrations, and number concentrations).

A discussion of the advantages and limitations of ZJU-AERO has been added, which can be found in Section 5 (Summary and Ongoing Tasks) of this paper:

"Currently, ZJU-AERO is an efficient forward radar operator that has the advantages of

handling complexities of non-spheroid particle models. Therefore, it is a powerful research tool for studying the sensitivities of polarimetric radar observations with respect to the non-sphericity of hydrometeor particles. It also applies parallel acceleration techniques to boost its performance, allowing operational applications of data assimilation in NWP models employing single-moment (SM) microphysics (such as CMA-GFS / MESO). ZJU-AERO forward radar operator can be applied in data assimilation (DA) studies using indirect DA methods such as Bayesian approach (Caumont et al., 2010) and direct DA methods such as Ensemble Kalman Filter (EnKF), which both requires no tangent-linear (TL) or adjoint (AD) versions of the forward radar operator.

ZJU-AERO also has some limitations. For example, it currently cannot be applied in DA research based on the variational method. Simplification and linearization works are involved to obtain a TL / AD version of the forward operator. Moreover, PSD solvers for DM microphysics schemes have already been implemented in ZJU-AERO for the experimental CMA-MESO DM microphysics, but there are many validation and evaluation works to be done. Also, unlike the EMVORADO, which uses a distributed-memory parallel design and interface with COSMO-NWP model online, ZJU-AERO applies a shared-memory parallel design and the NWP model input should be stored in external files."

2. In section 3.4, six SM microphysics schemes are used to explore the effects of different PSD schemes on the simulation of radar variables. It is not clear why the authors chose these six SM microphysics schemes. The shortcomings of the SM microphysics scheme are obvious in reproducing polarimetric features observed in convective storms and stratiform events. Although the SM microphysics scheme has been used for years and will continue to be used, the authors should clarify this point. Also, it is not clear that there are six schemes in Figure 11, while there are only five schemes in Figure 12 and three schemes in Figure 13. Based on the statistics in Figure 16, it seems that the Thompson or ThompsonTuned scheme has the best simulation results, and of course, the authors present only the results of the ThompsonTuned scheme in Figures 14 and 15. This is also clearly demonstrated in Figure 11. Therefore, is it necessary to evaluate other SM microphysics schemes?

Response: (1). Yes, it is necessary to clarify why we have chosen the six SM microphysics schemes for the sensitivity test in this study. Basically, we chose those schemes because they generally cover the natural variability of raindrop PSDs from continental precipitations (e.g., Wang2016) to maritime precipitations (e.g., Thompson 2008). Continental precipitations are characterized by having more large rain drops, while maritime precipitations have a larger population of drizzle-sized raindrops. We have added two paragraphs to address this issue in Section 3.4:

"According to global aircraft in-situ measurements carried out by Abel and Boutle (2012), the six single-moment (SM) microphysics assumptions in Table 3 cover the natural variability of raindrop PSDs ranging from continental precipitations to maritime precipitations. Typical continental PSD with intensive large drops such as Wang et al. (2016) and typical maritime PSD such as Thompson et al. (2008) with a large population of drizzle-sized raindrops are both present. That is why we have chosen the six SM

microphysics schemes for the PSD sensitivity test.

It should be noted that although SM microphysics has been used for years and will continue to be used, it has obvious shortcomings in reproducing polarimetric features observed in convective and stratiform events. Since double-moment (DM) microphysics in CMA-MESO is still experimental, the consistent DM scheme in ZJU-AERO is still in development stage. However, the nature variability of raindrop PSDs for DM microphysics schemes is still within what is displayed in Figure 10, therefore it is safe to use those SM assumptions for a sensitivity test."

(2). We agree that it is better to display the result of ThompsonTuned in Figure12. We added that to improve consistency:

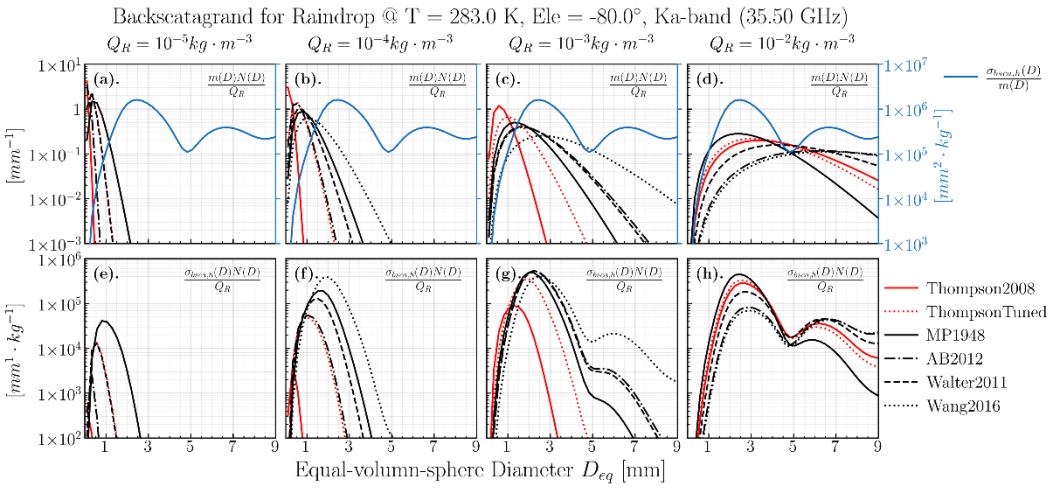

As for Figure 13, we only displayed the results of the SM PSD scheme MP1948, Thompson2008, and Wang2016, because displaying all 12 lines of 6 the schemes would make the figure too busy to read. MP1948 represents a traditional SM PSD scheme, while Thompson2008 and Wang2016 are representative of typical maritime and continental precipitation PSDs, respectively. We added sentences in captions of Figure 13 to justify the reason for omitting PSD schemes:

"Here, only the results of PSD schemes MP1948, Thompson2008 and Wang2016 are displayed, because MP1948 is a benchmark traditional PSD scheme, while Thompson2008 and Wang2016 are representative of typical maritime and continental precipitation PSD, respectively."

(3). As for whether it is necessary to evaluate other SM microphysics schemes, we believe the answer is positive. However, since there is a large degree of freedom for SM microphysics schemes, it is difficult to find a globally optimized SM microphysics assumption for all precipitation scenarios (stratiform and convective). Therefore, although we have found one locally optimized SM scheme for a tropical cyclone case through sensitivity studies, there is still much work to be done.

3. The authors describe a forward operator that can simulate ground-based and space-borne polarimetric radar observations, but only show the observation and simulation of the Ku-band radar reflectivity in the case study. This is clearly insufficient for proving the reliability of the forward operator. Simulated polarimetric radar variables (such as differential reflectivity, specific differential phase, and Co-polar correlation coefficient) should also be shown.

Response: Thanks for the suggestion, we have conducted a case study to simulate ground-based polarimetric radar variables using our forward operator. The simulation results demonstrate that our forward radar operator works properly in simulating ground-based polarimetric variables and generally agrees well with previous radar simulators.

The results of the case study are displayed in Figure 2 and Figure 3 of this response letter, which can also be found in the user manual of the radar operator (released together with the software package).

From Figure 2 and Figure 3, it can be observed that the SM PSD scheme in the simulation tends to overestimate the large drops in this heavy precipitation event, resulting in larger simulated ZDR values (see Figure 2b) compared to the observed values in Figure 3b. It is known in the field of qualitative precipitation estimations (QPEs) that heavy precipitation events with tropical maritime characteristics tend to have more smaller drops and larger precipitation rates for a given reflectivity value (e.g., 50 dBZ). The low ZDR value (~1dB) accompanied by large reflectivity values (> 50dBZ) in the liquid phase indicates extremely large precipitation rates contributed by intensive small drops. This cannot be accurately described by a SM microphysics parameterization.

Overall, the simulation results produced by ZJU-AERO using the SM microphysics input for ground-based polarimetric variables are reasonable. However, more research is needed to accurately reproduce the melting layer features observed in Figure 2b and 2c.

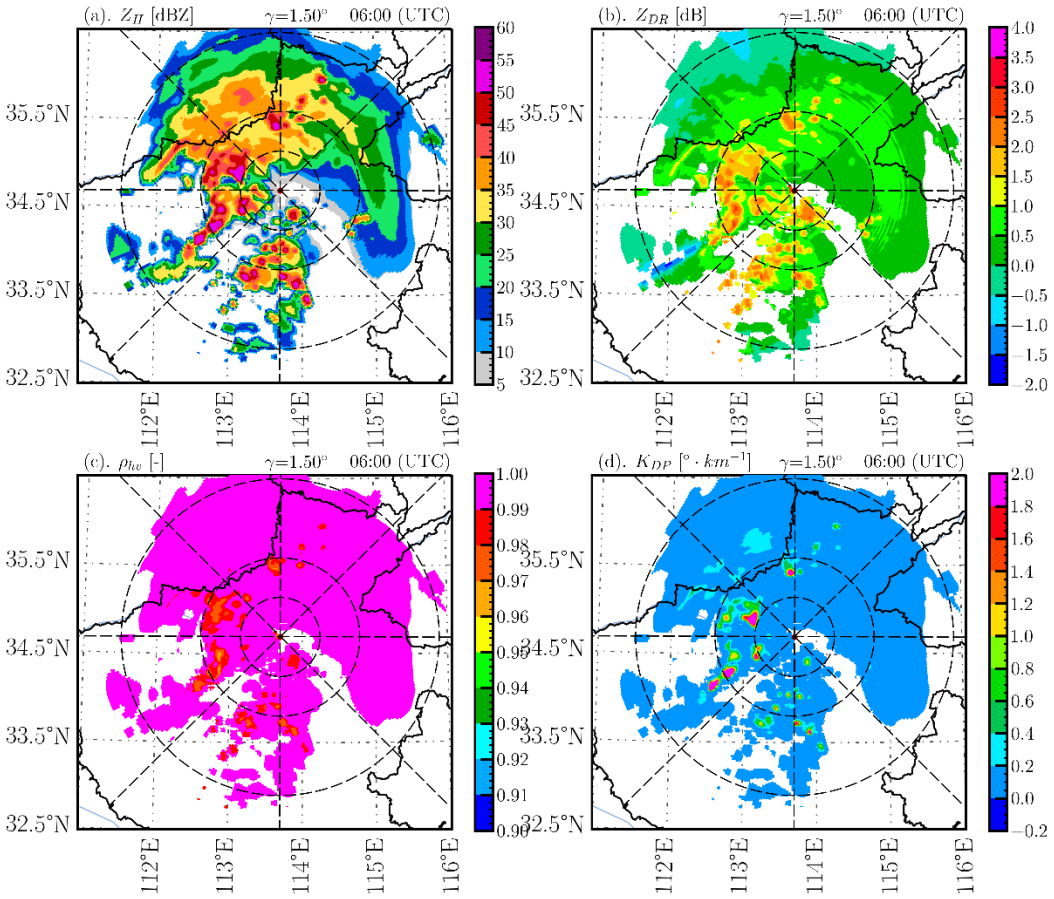

Figure 2: The simulated polarimetric radar variables of a PPI snapshot (elevation angle=1.5 deg.) for a meso-scale convective system (MCS) recorded with heavy precipitation event in Henan Province, China. The observation was performed by CINRAD 98DP S-band Radar of Z9371 Zhengzhou site at 6:00UTC on July 20, 2021. All the radar operator simulations were conducted based on the T+6H forecast model grid data of WRF using the Thompson microphysics scheme, which was initialized at 00:00 UTC on July 20, 2021. We used default settings in ZJU-AERO (spheroid particle models and microphysics-consistent PSD solvers).

Considering the current length of this manuscript, we have added those simulation results in the user manual of the software (which was released together with the software package) instead of including them in the research paper. That is because the simulation results are relatively trivial compared to previous radar operators, and there are no significant scientific issues that require documentation:

We have added the following statement in the introduction of Section 4:

"To demonstrate the reliability of the forward radar operator for ground-based polarimetric radars, we have also performed a case study of a meso-scale convective system (MCS), which can be found in the user manual (see Section Code Availability). The results are reasonable but relatively trivial compared to previous radar operators, so we will not display them in this section."

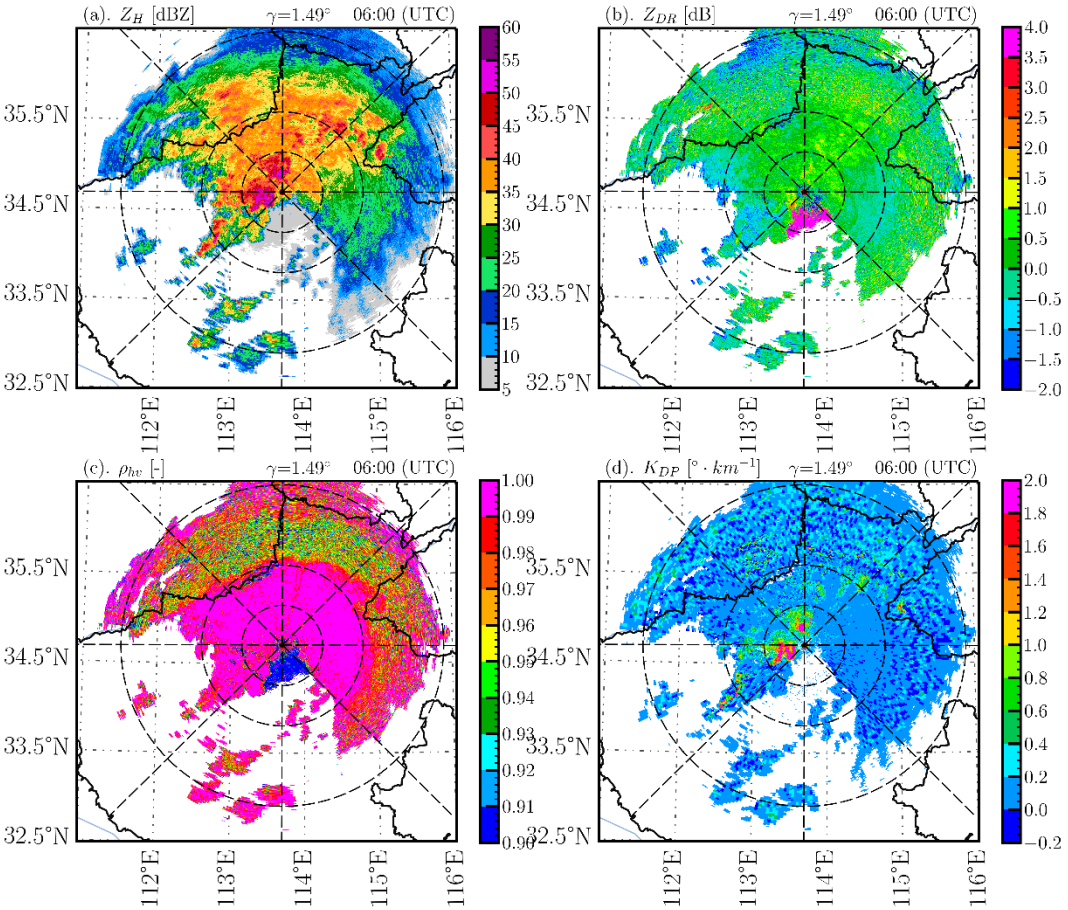

Figure 3: The observed polarimetric radar variables of a PPI snapshot (elevation angle=1.5 deg.) for a meso-scale convective system (MCS) recorded with heavy precipitation event in Henan Province, China. The observation was performed by CINRAD 98DP S-band Radar of Z9371 Zhengzhou site at 6:00UTC on July 20, 2021.

4. There are some concerns about the value of introducing the Chebyshev-shaped model for raindrops. In Figure 13, it is shown that the ZDR simulated by the Chebyshev-shaped model and the spherical model in the Thompson scheme only show a pronounced difference when the liquid water content is larger, and the differences in the other radar variables are very small. Figure 16 shows that the Chebyshev-shaped model and the spherical model have the same simulation distributions on radar reflectivity. It's not clear if ZDR would have a different result. This goes back to the previous comment. In addition, whether there would be a difference between the Chebyshev-shaped model and the spherical model if the statistics were performed at different locations of the typhoon.

   Response: (1). Thanks for the suggestion. Further discussions regarding the value of introducing Chebyshev-shaped model for raindrops are necessary.

   Based on our findings, the deviations between the Chebyshev and Spheroid models (indicated as CmS) are prominent only for Ku-, Ka-, and W-band radars, and for large drops (Deq>5mm) at zenith and nadir viewing geometries (see Figure 8 in the manuscript).

To explore the sensitivity of spaceborne radar (Ku- and Ka-band) observed reflectivity with respect to the shape of raindrop model at extreme scenarios when large drops dominates, we have conducted observation system simulation experiments (OSSEs) (see Figure 4 - Figure 7).

We assumed an imaginary spaceborne radar GPM-DPR overpass for the MCS event discussed in Figure 3 and performed simulations for both Chebyshev and Spheroid raindrop particle model settings.

Figure 4 shows that assuming raindrops as Chebyshev-shape rather than spheroids can lead to a decrease in simulated reflectivity for more than 1 dB in heavy precipitation regions (Figure 4i). This is also true for Ka-band if no instrument sensitivity mask (12 dBZ) is applied, and the CmS reflectivity can be even larger (more than 2 dB, see Figure 5i, which is consistent with Figure 13a in the manuscript).

This decrease is due to the fact that the top of large Chebyshev raindrops tends to have much lower backscattering cross-section than Spheroids (Figure 8a in manuscript), and the extinction cross-section of large Chebyshev raindrops is slightly higher than spheroids (Figure 8b in manuscript). These two effects reinforce each other, resulting in lower simulated reflectivity for the Chebyshev experimental group.

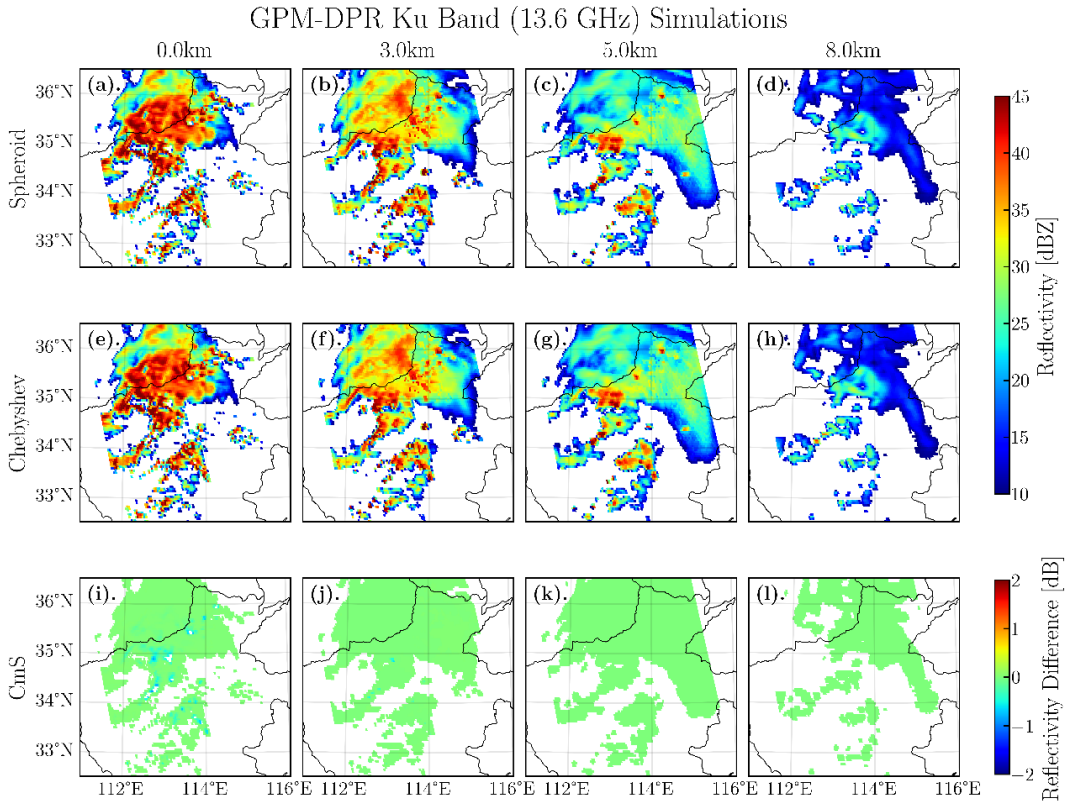

Figure 4: Results of Ku-Band (13.6 GHz) OSSE raindrop particle model sensitivity test. The first row displays the simulated reflectivity assuming spheroid raindrops, while the second row displays those assuming Chebyshev-shape raindrops. The final row displays the Chebyshev – Spheroid (CmS) deviations of reflectivity. The four columns of panels display the simulation results at different altitudes, among them the first (0km) and second column (3km) is pure liquid phase. The case is the same MCS

event as that in Figure 1, but “forced” continental DSD scheme “Wang2016” is used to explore the extreme CmS sensitivity when large drops dominate.

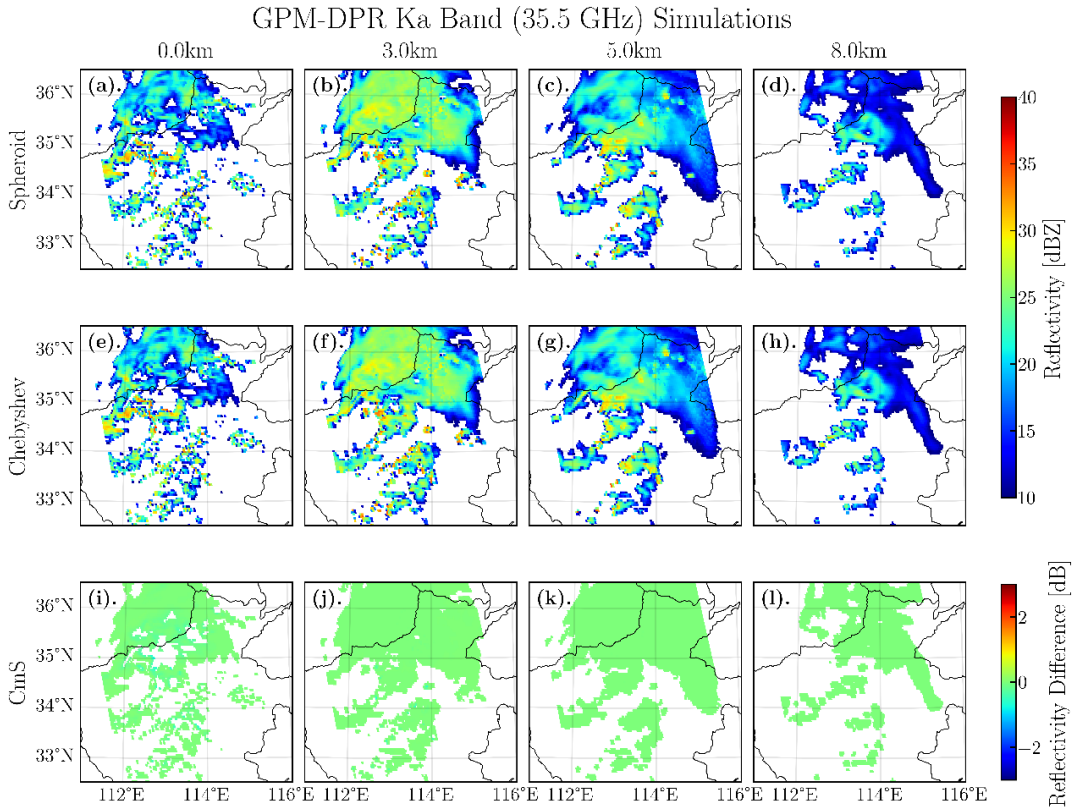

Figure 5: Results of Ka-Band (35.5 GHz) OSSE raindrop particle model sensitivity test. Similar with Figure 4.

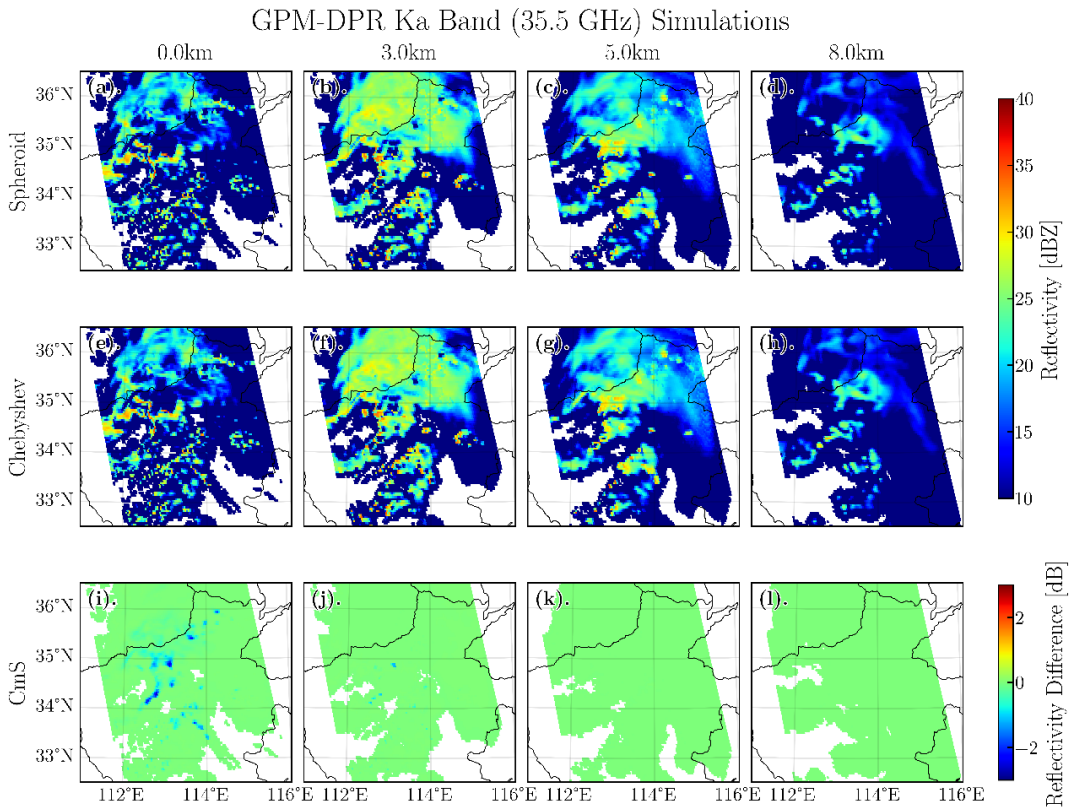

Figure 6: Similar with Figure 5 but no instrument sensitivity threshold (12dBZ) is applied to the simulation results.

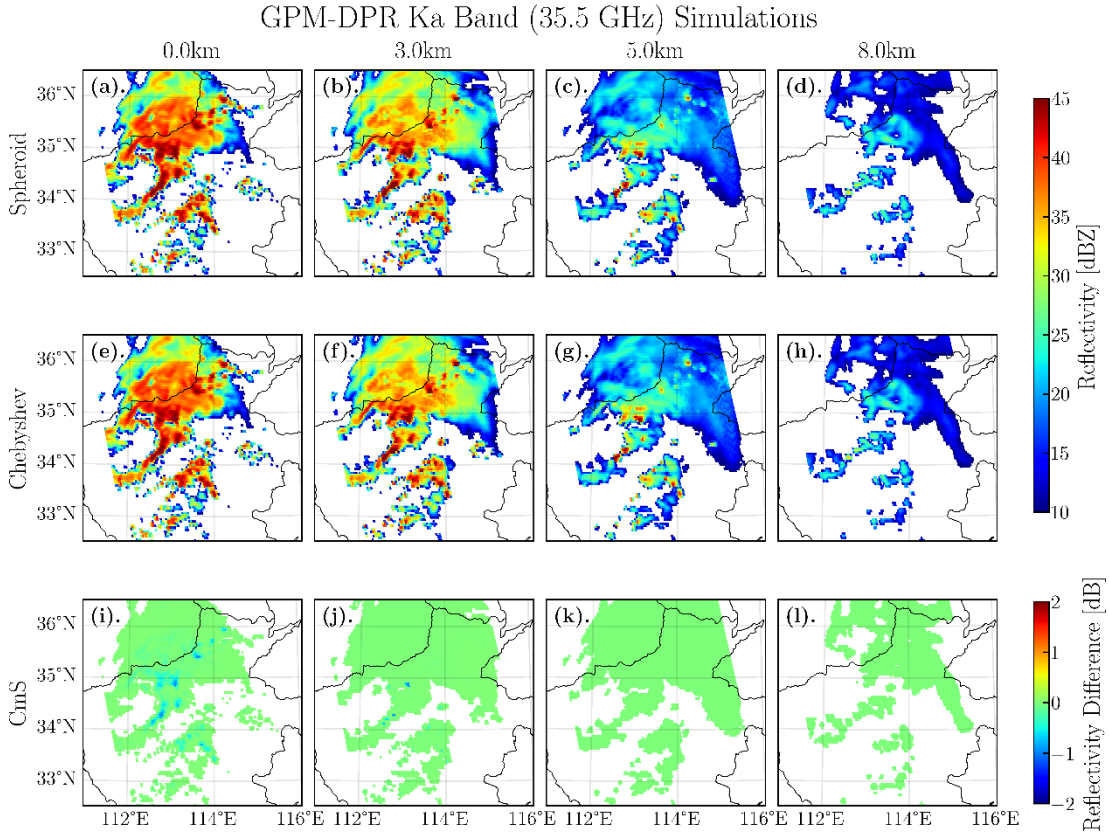

Figure 7: Similar with Figure 5 but no attenuation effect is considered.

However, if the instrument sensitivity mask is applied for Ka-band (see Figure 5), then the observed reflectivity of liquid layer in heavy precipitation regions falls below the instrument sensitivity threshold and becomes invisible. This is because heavy precipitation regions tend to have much higher path-integrated attenuation (PIA), which makes the large negative values of CmS in the lower liquid phase (see Figure 5i) invisible. This does not mean that the CmS effect is not important for Ka-band; it can have significant effect for vertical pointing (VP) ground-based radars and airborne radars (looking from beneath or inside liquid clouds), for which the raindrops in heavy precipitation regions can be visible since the PIA can be much smaller.

In summary, the Chebyshev-shape raindrop model can have significant effects in certain scenarios, as observed in our OSSEs. However, the CmS effect shows little difference for the ThompsonTuned scheme (Figure 16 in the manuscript) because small drops dominate in this PSD scheme.

(2). Regarding the ZDR difference, it is only prominent for side-viewing geometry (elevation angle ~ 0 deg.), as the ZDR signatures of precipitation particles diminish for nadir and zenith viewing geometries. Therefore, we need to inspect the Look-Up Tables (LUTs) of Chebyshev-shaped raindrops at an elevation angles of 5 deg. and Ka-band.

Figure 8 shows that the ZDR difference between the Chebyshev-shape and spheroids at side-viewing geometry is small, only prominent for several narrow diameter bands when oscillation occurs. Consequently, for ground-based radars working at lower-frequency bands (S/ C / X-bands, figure not shown), the CmS effect for polarimetric variables is negligible.

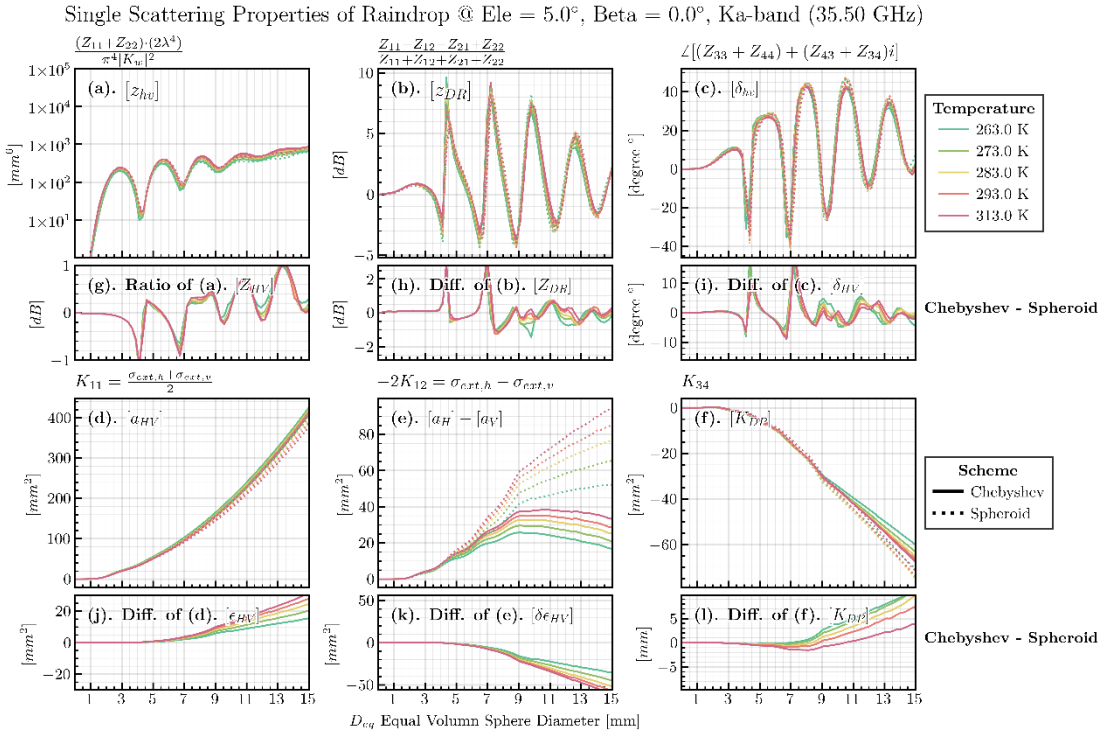

Figure 8: The single scattering properties of Chebyshev shapes and Spheroid shapes at side viewing

geometry (for ground-based radars) at Ka-band (35.5 GHz).

This study is not only about presenting an alternative raindrop particle model in forward radar operator, but it also demonstrates the capability for ZJU-AERO to handle the complexities of non-spheroid particle models. Similar research will soon be applied to other types of hydrometeors, such as melting and solid particles. The potential for improvement when applying complex non-spheroid models for melting and solid particles should be much higher than for raindrops.

(3). Based on the above discussions, we expected that if statistics are performed in different regions of a tropical cyclone, the differences between Chebyshev-shape and Spheroid raindrop particle models tend to be minimal, because small drops dominate in this case. We have conducted sensitivity tests for different PSD schemes in different regions of the tropical cyclone (core region and outer spiral rainbands), as shown in Figure 9 - Figure 11. The core region is marked in Figure 9, while the outer precipitation regions are recognized as outer spiral rainbands. In both the core region and outer spiral rainbands of the tropical cyclone, the ThompsonTuned PSD scheme provided the best fit in Figure 10 and Figure 11.

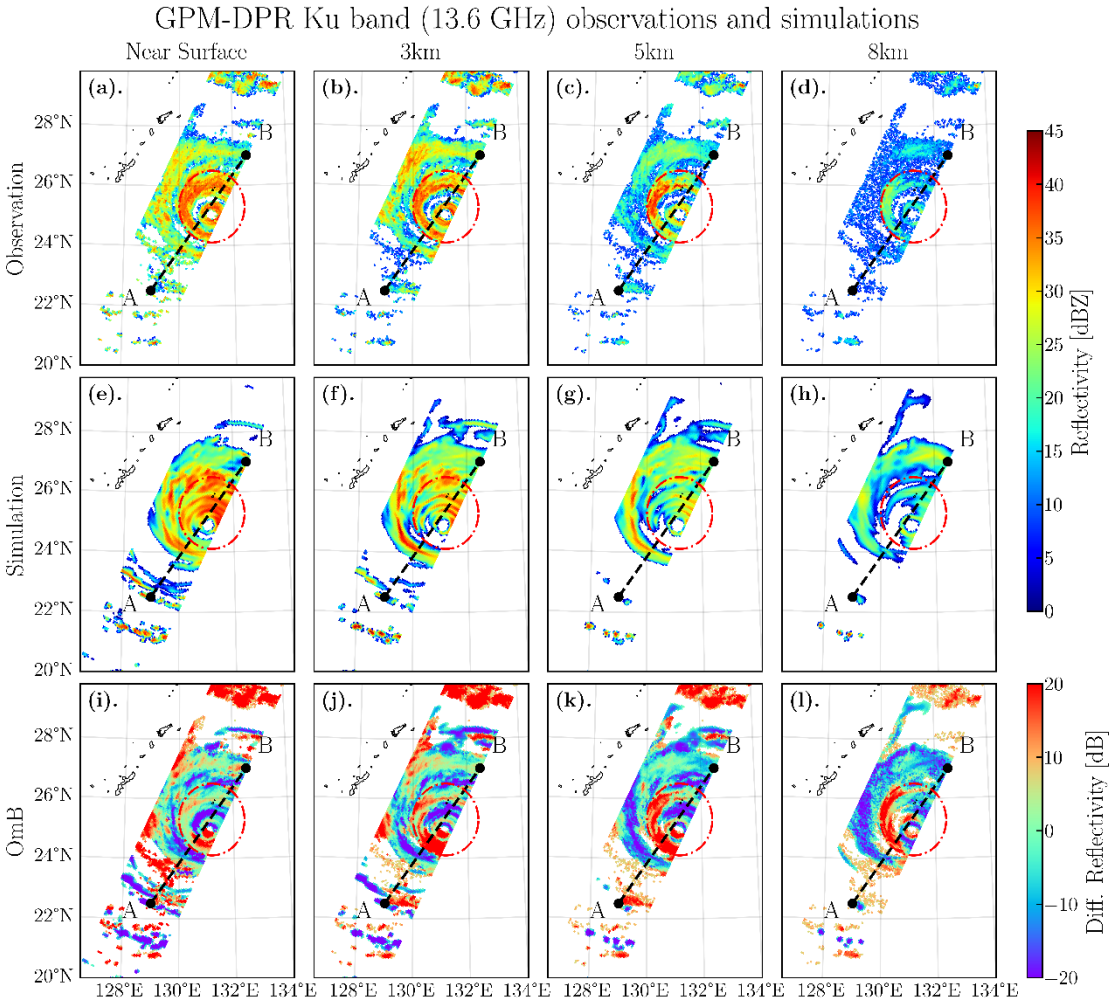

Figure 9: Same as Figure 14 in manuscript, but region mask is added for tropical cyclones cores (the region within the red dash-dotted cycle). The out spiral rain bands of tropical cyclone are recognized as regions beyond the dash-dotted cycle.

Therefore, we have added these discussions to the final paragraph of Section 4.2:

"…… An observation system simulation experiment of GPM-DPR overpassing a meso-scale convective system (recorded with extreme heavy precipitation events) reported CmS decrease effects of more than 1 dB at Ku-band and more than 2 dB at Ka-band (figures now shown). This sensitivity test is consistent with what we found in Figure12(a) and demonstrates the importance of introducing Chebyshev-shape raindrop model in certain scenarios (e.g., vertical pointing cloud radar, airborne radar and spaceborne radar working at high-frequency bands). As for polarimetric radar variables such as Z_{DR} and K_{DP} for ground-based radar at side-viewing geometry, the CmS effects are generally negligible."

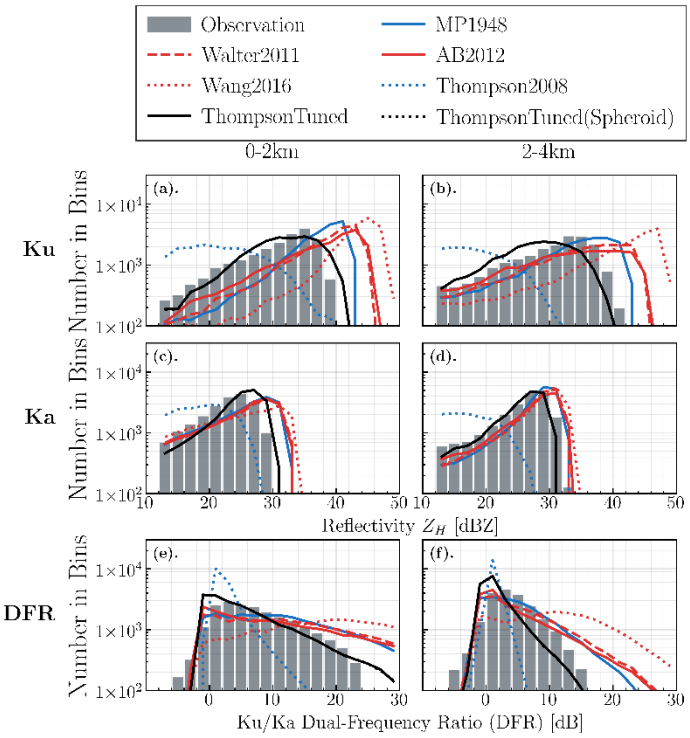

Figure 10: Similar with Figure 16 in manuscript, but only observations in tropical cyclone core (see Figure 9) are used for statistics.

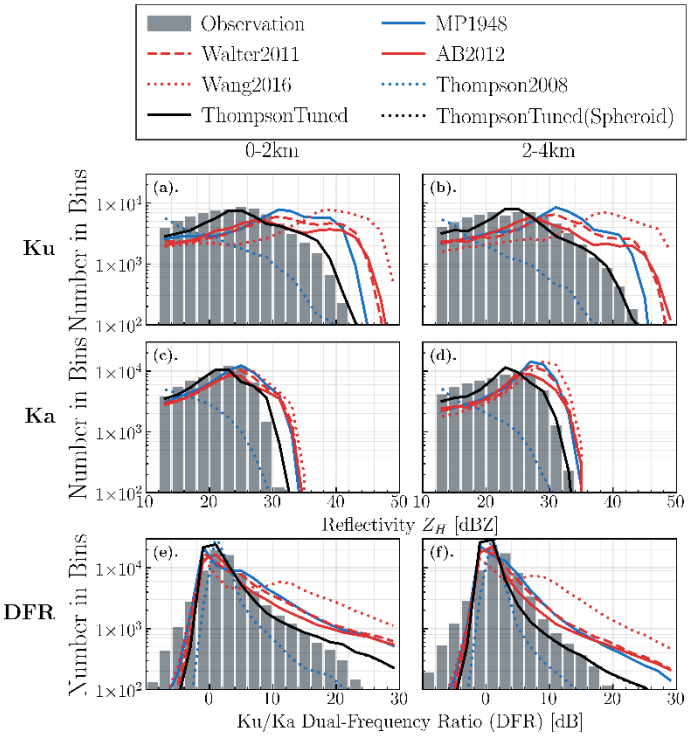

Figure 11: Similar with Figure 16 in manuscript, but only observations in tropical cyclone outer spiral rain bands (see Figure 9) are used for statistics.

Minor comment:

1. Title: I suggest that the name of the operator would be used the words that more objectively, characterized the operator, instead of some subjective adjectives like “accurate and efficient”.

Response: Thank you for your suggestion. After careful considerations, we have decided not to change the title. This software has already been used by several research groups in China, and we have other research papers currently under review using the same software name.

2. L17: which the Doppler variables are meant here?

   Response: Here, Doppler variables refer to radial velocity (VRAD) and spectrum width (WRAD).

   "……, excluding the Doppler variables such as radial velocity and spectrum width."

3. L125: Qh (hail) is included in Figure 2, but not here. Please be consistent.

   Response: Thank you for pointing that out. Hail has not been implemented in the current version, so Qh has been removed from Figure 2 in the manuscript to maintain consistency.

4. L195: "…undergone sufficient discussions in other works concerning radar operators, and we just inherited those settings and options from them", please add specific references.

   Response: Thank you for your feedback. We have added specific references to support this statement:

   "In this paper, we do not elaborate on the algorithm details of certain issues, such as (a) trilinear interpolation, (b) sub-beam sampling and antenna pattern weighted averaging, and (c) ray-tracing trajectory solver. For trilinear interpolation, we follow the approach described in Wolfensberger and Berne (2018) to interpolate the model grid data to radar gates of each sub-trajectory gridpoint. Regarding sub-beam sampling and antenna pattern weighted averaging, we utilized Gauss-Hermite quadrature as outlined in Caumont et al. (2006). As the ray-tracing trajectory solver, we offer users both an offline beam trajectory solver (4/3RE) and an online beam trajectory solver (Zeng et al., 2014). All of these methods are reimplemented in Python, using either efficient numpy/scipy API or customized cython extensions."

5. L229: Z and K are very critical variables, and their specific definitions should be given.

   Response: Thank you for your suggestions. We have provided specific definitions for matrix Z and K:

   "Apart from the 2×2 complex amplitude scattering matrix S defined on complex electric field vector bases, one can define the 4×4 real matrix, known as the Mueller matrix, Z, and extinction matrix, K, which describe polarimetric light scattering and extinction properties of particles on the real Stokes vector bases, respectively. We kept the definitions of Z and K consistent with those mentioned in a study by Mishchenko (2014):

$$\mathbf{I}^{sca}\left(r\hat{\mathbf{n}}^{\mathbf{sca}}\right)=\frac{1}{r^2}\mathbf{Z}\left(\hat{\mathbf{n}}^{\mathbf{sca}},\hat{\mathbf{n}}^{\mathbf{inc}}\right)\mathbf{I}^{inc}, \quad (3)$$

$$\mathbf{I}\left(r\hat{\mathbf{n}}^{inc}\right)\Delta S=\mathbf{I}^{inc}\Delta S-\mathbf{K}\left(\hat{\mathbf{n}}^{inc}\right)\mathbf{I}^{inc}+O(r^{-2}), \quad (4)$$

Eq. (3) and (4) give the definitions of Mueller matrix Z and extinction matrix K, respectively. Here, $\mathbf{I}^{sca}$ and $\mathbf{I}^{inc}$ represent the Stokes vector $[I, Q, U, V]^T$ of scattering and incident light, while the unit vectors $\hat{\mathbf{n}}^{\mathbf{sca}}$ and $\hat{\mathbf{n}}^{\mathbf{inc}}$ indicate the unit vectors of directions of scattering and incident light, respectively. r is the distance of detector from the particle,

while ΔS *is the receiving surface of detector aligned normal to and centered on the straight line extending from the particle in the direction of the unit vector* $\hat{\mathbf{n}}^{\mathbf{inc}}$. $O(r^{-2})$ *in Eq. (4) represents that the forward scattering term decreases by the inversed square law."*

6. Eq. (5): It is suggested that Zh and Zv be separated into two formulas. The plus and minus signs are very confusing here.

   Response: Done.

7. L398: "…incident radar beam and OZL This alignment sets the azimuthal…" should be "…incident radar beam and OZL. This alignment sets the azimuthal…"

   Response: Yes, a missing "." is added now.

8. L411: How to determine if a particle is axial symmetric in the program.

   Response: Basically, the axial symmetry is determined before calculating scattering properties database (LUTs) for a specific particle model, such as the Chebyshev-shape raindrop and hexagonal ice crystals.

   For example, the dielectric constant distribution of electromagnetic medium $\varepsilon(\theta,\varphi,r)$ in spherical coordinates is not relevant with the azimuth angle φ for Chebyshev-shape raindrops, but it is relevant with azimuth angle φ for hexagonal ice crystals, which only have 6-fold azimuthal symmetry. Consequently, we can conclude that Chebyshev-shaped raindrops have axial symmetry while hexagonal ice crystals do not, based on mathematical expressions rather than a computer program.

   We added specifications to make the statement clearer:

   "……For both axially symmetric (i.e., the dielectric constant distribution of electromagnetic medium in spherical coordinates $\varepsilon(r,\theta,\varphi)$ *is irrelevant with azimuth angle* φ*)……"*

9. L456: "It is apprarent" should be "It is apparent"?

   Response: Yes, typo is fixed now.

10. L564: Why use a constant air density instead of diagnostic air density. Air density decreases with increasing altitude, it also changes with variations in pressure, temperature, and humidity.

    Response: Yes, we did not specify the point clearly here: the constant air density is only used in determine the position of N_0-λ curve of Figure 11 in the manuscript. That is because if diagnostic air density is considered, then we cannot determine the N_0-Λ curve in Figure 11 (the position of N_0-Λ curve depends on Q_{R0} expressed as mass concentration rather than mixing ratio). That means constant air density is only used in qualitative diagnose of N_0-Λ curve plot, while in real PSD solver of ZJU-AERO, the diagnostic air density is used.

    Notes have been added to the caption of Table 3 in the manuscript:

    "……It should be noted that the constant air density is only used here to qualitatively determine the position of the Thompson2008 and ThompsonTuned N0- Λ *curves in Figure 11. Diagnostic air density is used in actual PSD solver of ZJU-AERO."*

11. L684: Why does not it show the temperature profile? There is no temperature profile how to determine the altitude of freezing level.

    Response: Yes, thanks for the suggestion. We have added Isothermal lines

of model background state to each panel of Figure 15 to show the temperature profile. The red isothermal line at 0℃ indicates the freezing level.

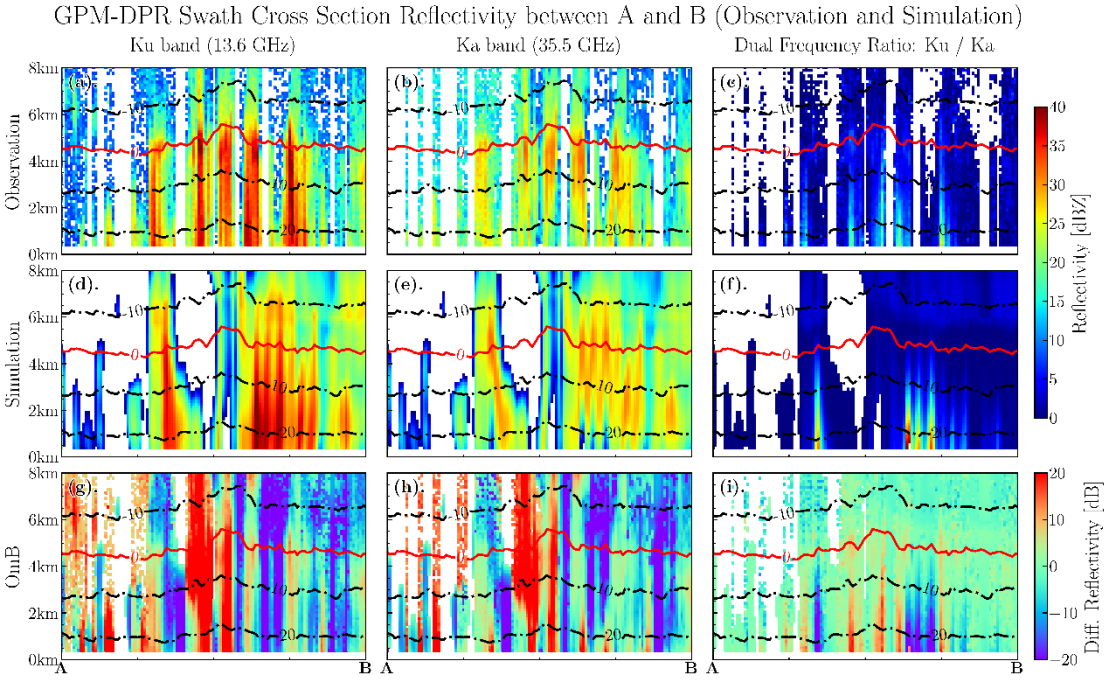

Add in description in caption of Figure 15:

"…… The temperature of model background state is indicated by isothermal lines in each panel. Numbers of the contour labels have the unit of Celsius degree."

12. L686: It is difficult to see the features of the melting layer in Figure 15a and b.

    Response: We acknowledged that the features of melting layer are weak at Ku-band and not prominent at Ka-band for this case, where the precipitation system is not so horizontally homogeneous. We updated the descriptions in the manuscript accordingly:

    "Actually, the GPM-DPR observations revealed a weak bright band (BB) signature below the freezing level, which can be recognized at Ku-band (with an average reflectivity enhancement of approximately 3 dB, see Figure 14a) but not so clear at Ka-band (see Figure 14b)."

13. L690-692: This may be due to the operator not considering melting or mixed-phased particles, and the shortcoming of the microphysics scheme.

    Response: Yes, the reason why ZJU-AERO cannot simulate melting layer signatures is rearranged as follows:

    "However, the simulations we conducted did not show an obvious BB, which was attributed to not considering melting or mixed-phased particles, and the shortcoming of the microphysics scheme."

14. Figure 15: It is suggested to add temperature profile.

    Response: We have added the temperature profile in Figure 15 by including isothermal lines (see response to minor comment 11).

15. The SUMMARY is not sufficient.

    Response: Thanks for the suggestions. We have expanded the summary

section and make it complete:

"In summary, Section 2 of our study introduced the basic concepts of design and formulations in the ZJU-AERO. These concepts included the general procedure of the software, radar variable calculations, and the available hydrometeor settings (shape parameters, dielectric constant models, canting angles, particle size distributions). We also derived the formulation of polarimetric radar variables starting from single particle back-scattering Muller matrix Z and extinction matrix K.

In Section 3, we highlighted the unique features of ZJU-AERO, specifically its multi-layered design for the optical database of non-spherical particles. We demonstrated this by visualizing the scattering properties using the example of the Chebyshev-shape raindrop particle model, comparing it to the properties of traditional spheroid raindrops. We conducted LUT demonstrations for two database layers: Level-A (raw single scattering properties database), and Level-C (bulk scattering property database). We also introduced a new intermediate quantity named as "backscatagrand" to diagnose the PSD integrations of optical properties. We concluded that the Chebyshev-shape raindrop model shows noticeable differences of bulk scattering properties (compared to spheroid model) only at zenith and nadir viewing geometries and for milimeter-wavelength radar bands. This difference is more prominent for continental DSD models (e.g., Wang2016) with larger drops. These deviations can reach up to 2-3 dB at Ka-band for spaceborne radars in heavy continental precipitation regions where large drops dominate. Given the lower uncertainties in simulating reflectivity of liquid phase compared to solid and melting phases, such a difference deserves attention in specific applications such as comparing data from ground-based and spaceborne radar observations (Warren et al., 2018).

Furthermore, in Section 4, we validated the simulation reliability and capability of ZJU-AERO by analyzing a case study of a tropical cyclone using input from the CMA-MESO for simulating spaceborne radar observations. We found that ZJU-AERO provides reasonable simulation results, except for the bright band signature at melting layer, which can be attributed to the current version of ZJU-AERO, not considering melting or mixed-phased particles. We also performed sensitivity assessments of PSDs and morphology options in ZJU-AERO and found that the ThompsonTuned single-moment PSD scheme provides the best fit of the reflectivity histogram in the simulation to the GPM-DPR observation. However, using either the Chebyshev-shaped raindrop particle model or the spheroid model makes little difference to the simulation results since the tropical cyclone precipitation has a maritime DSD, where small drops dominate."